3D X-ray Microscopy (XRM) investigation of exogenous materials inside mussels' organs

3D X-ray Microscopy (XRM) investigation of exogenous materials inside mussels' organs

F Cognigni[1], S Dinarelli[1], M Girasole[2], G Longo[2], G Fabi[3] and M Rossi[1,4]

[1] Department of Basic and Applied Science, Sapienza University, Rome, Italy
[2] Institute for the Structure of Matter, National Research Council, Rome, Italy
[3] Institute for Biological Resources and Marine Biotechnology, National Research Council, Ancona, Italy
[4] CNIS - Center on Nanotechnology Applied to the Engineering of Sapienza, Sapienza University, Rome, Italy

E-mail: simone.dinarelli@uniroma1.it

Abstract. The diffusion of pollutants in the marine environment is nowadays a well-recognized issue that is attracting growing interest from the scientific and social communities. One of the possible strategies to study the effect of pollutants is to quantify their presence inside marine organisms that are directly exposed for a certain period to the polluted environment. Among them, mussels, commonly considered as "biological water filters", stand out as ideal candidates since they are stationary animals and their food intake comes only from the filtering of the surrounding water. Thus, the evaluation of the accumulation of exogenous pollutants, in particular high-density or metallic, inside the mussel's organs and specifically in its digestive glands, is of particular interest. In this paper we characterize the accumulation of exogenous materials in digestive glands of three different mussels by means of X-ray microscopy analysis. We provide evidence of how the unique capabilities of this technique allow reconstructing a full 3D image of an entire organ and how this image can provide valuable information to identify exogenous (non-biological) pollutants. Moreover, we take full advantage from the segmentation analysis of the images by discriminating different regions of the sample according to the density. With this experimental approach we measured the sizes of the exogenous pollutants and provided evidences that they accumulate preferentiality in the low-density regions of the organ, that are richer in ducts and secretive glands.

Key words: mussels, exogenous pollutants, X-ray microscopy

1. Introduction

The diffusion of pollutants, of different origins and composition, in the marine environment is gaining growing interest in the scientific community over the last years. The study of these contaminants and of their effects on the biota is paramount to define strategies to mitigate such effects. This is particularly true for high-density or metal-based pollutants which bears the highest harmful potential for ecosystems and biosystems. Among the many studies focused on these interactions, the investigation of samples collected directly from the marine environment are the most challenging, since the abundance and chemical composition of the pollutants are difficult to be defined [1, 2]. In the marine environment, the biological activity of pollutants depends on several factors, such as composition, chemical stability, structure, surface chemistry and presence of concomitant additional surfactant. In addition, the fate of pollutants inside a marine organism can be very different. A pollutant can be simply accumulated without generating harmful effects on the animal; it can induce biological modifications in cells, tissue

or organs leading to the impairment of several functions; or can be neutralised and expelled from the organism itself. All these factors are affected by toxicity and accumulation rate at the level of tissue or entire organ [3,4]. Among the various organisms that can be studied, mussels (*Mytilus galloprovincialis*) are the ideal candidates for studies of pollution in marine environments since they are stationary animals and can be considered as natural water filters since their food intake comes from filtering the surrounding water. Nonetheless, mussels are edible organisms and can easily transfer the pollutants accumulated during their life through the food chain directly to humans. For this reason, the investigation of pollutants inside mussel's organs can be a reliable and direct way to monitor marine pollution. Several studies are available on the effect of pollutants on mussels [5,6], making use of different techniques, from biochemical characterizations [7-9], to spectroscopies [4] or even high-resolution microscopies such as Scanning Electron Microscopy (SEM) and Atomic Force Microscopy (AFM) [10]. Every given technique presents its own advantages and limitations in terms of balance between resolution, localization capabilities, quantity of material sampled and how much the sampled region can be representative of the entire animal or organ. A recently developed technique that holds the promise to be particularly useful in this field is X-ray Microscopy (XRM) that delivers a non-destructive characterization providing internal microstructural and compositional information about the sample and is particularly suitable for a multiscale and multimodal 2D/3D approach [11,12]. XRM is becoming increasingly popular thanks to its ability to reveal internal details of even large samples without the need of sectioning or dismantling, which can be a crucial advantage, especially in the case of biological samples. The experimental setup is typically composed of three main elements: (i) a source that produces the X-ray beam, (ii) a charge-coupled device (CCD) detector that collects the transmitted X-rays and (iii) a rotating sample stage, placed between the source and the detector, which firmly holds the sample in the desired position and ensures its controlled rotation during the analysis [13]. The contrast obtained in the final image strongly depends on the X-ray absorption phenomenon that occurs along the X-ray beam path (L) inside the sample, it is function of the attenuation coefficient value (x) in a certain position (dx) of the specimen and depends on the intensity of the X-ray beam before entering the sample (I_0). These parameters are related by the Beer-Lambert law:

$$I_L = I_0 e^{-Lxdx} \quad (1)$$

where I_L represents the transmitted X-ray beam intensity. Equation 1 describes the exponential decrease of a quasi-monochromatic X-ray beam passing through a heterogeneous object [13,14]. The transmitted X-ray beam reaches the detector where it is converted into visible light through a scintillator and the signal is then recorded and magnified by a camera. This is the process that leads to the acquisition of a single projection image and it is repeated iteratively over many different rotation angle values with respect to the X-ray beam direction, until a complete set of projection images is obtained [13,15]. A tomographic reconstruction algorithm is then used to obtain the 2D/3D reconstruction of the object from this set of projection images. Generally speaking, an X-ray Microscopy experiment can be run in two different modalities: absorption contrast tomography or phase contrast tomography. The first method allows to obtain the bi- and three-dimensional imaginary part of the refractive index distribution of the specimen, which is sensible to the X-ray amplitude changes. On the other hand, the second method is related to the change in wavelength of the X-ray beam along its path through the sample and measures the real part of the complex refractive index of the object. Although the phase contrast tomography is particularly suitable for low-Z materials such as polymers or biological samples that typically show a weak absorption [16,17], in this work the physical dimensions of the samples allowed us to work in absorption contrast tomography, thus being more sensible to the internal details of the structures. This work follows on the footsteps of previous works [9,10] that were devoted to the identification, with high resolution techniques, of nano and micro-sized pollutants in tiny sections of mussels. Through X-ray tomography, we can add quantitative and localized information of the exogenous pollutants, providing a micron scale map at the level of entire organs.

2. Materials and Methods

2.1. Sample collection and organs extraction

The mussels (*M. galloprovincialis*) analysed in this work were part of a more comprehensive study, whose complete set of information can be found in [9]. Briefly, the collected animals were rapidly transported in cold boxes in laboratory to perform the extraction of the digestive glands, which were subsequently dissected, cut in sections of 1 to 2 mm and then immersed in 2,5% glutaraldehyde phosphate buffer 0.2M solution with pH 7.2 and stored at 4°C until the resin embedding procedure.

2.2. Resin embedding procedure

The embedding procedure followed an already established protocol described in detail in [10]:

- 3x washes in Buffer Phosphate
- post-fixation in Osmium Tetroxide 1% for 8 hours
- 3x washes in Buffer Phosphate
- 2x exposure of 10 minutes each in solutions at growing concentration of Ethanol (from 25% up to 100% EtOH)
- 3x washes in Buffer Phosphate
- substitution of EtOH with a solution of 50% Propylene oxide for 10 minutes
- 2x passages in pure Propylene oxide solution for 20 minutes each

After this passage, the samples were cut in small pieces with a surgical knife and the resin embedding (Multilab 812 resin kit) was performed by exposing the samples to solutions with progressive concentration of resin increase in steps (from 33% to 100% resin).
The resin polymerization procedure (48 hours at 60°C) was performed after 1 hour from the exposure to pure resin, resulting in epoxy blocks, which were ready to be analysed with the 3D-Xray tomography without further processing.

2.3. X-ray Microscopy (XRM)

X-ray Microscopy analysis was performed using a laboratory X-ray microscope (Zeiss, Xradia Versa 610) at Sapienza Nanoscience & Nanotechnology Laboratories (SNN-Lab) of the Research Centre on Nanotechnology Applied to Engineering (CNIS) of Sapienza University of Rome. When scanned, the specimens were glued on a pencil lead and then fixed on the sample stage by the Pin Vise sample holder. The sample stage stands between the X-ray source and the detector and can rotate around a fixed axis to ensure a full 360° scan. For all the three samples the voltage and power of the X-ray beam were 50 kV and 4.5 W, respectively, the scans were performed from 0° to 360° using a 4x objective, acquiring 3201 projection images binned 2x2x2. The relative distances (sample-to-detector and sample-to-source) as well as the exposure time, were adjusted in such a way to optimise the signal-to-noise ratio and obtain a pixel size of 2 μm and then a voxel size of 8 μm^3. The total scanning time for the three samples changes accordingly to these parameters from around 9 hours up to 11 hours.

2.4. 3D models Reconstruction

3D models were reconstructed using the Reconstructor module of Zeiss Scout and Scan control software - Zeiss (Version 16.1.13038.43550) by which reconstruction parameters such as Centre Shift and Beam Hardening Constant were identified. At the end of the process a TIFF stack was obtained and subsequently imported in Dragonfly Pro software (Version 2020.1 Build 797, Object Research System) for post processing. Dragonfly Pro was used to (i) visualise the samples excluding the signal coming from the air around the specimens through the window levelling tab, (ii) generate the images presented in this paper and (iii) perform the segmentation procedure of the samples thus obtaining the sizes of the exogenous material. The subsequent data analysis of these sizes was performed with the Software OriginPro 2018.

3. Results and Discussions

Tomographies were collected from digestive gland samples from three different animals. The digestive glands are the organs responsible for the extraction of nutrients from the filtered water, essentially all the water that was filtered by the animal will pass through the ducts, glands and connective tissue that compose this organ. probably, most of the exogenous material that interacted with the tissue and was not expelled is stored in this organ, which is consequently expected to uptake an amount of pollutants greater than any other organ of the mussel. In figure 1, a complete tomography of a sample is reported.

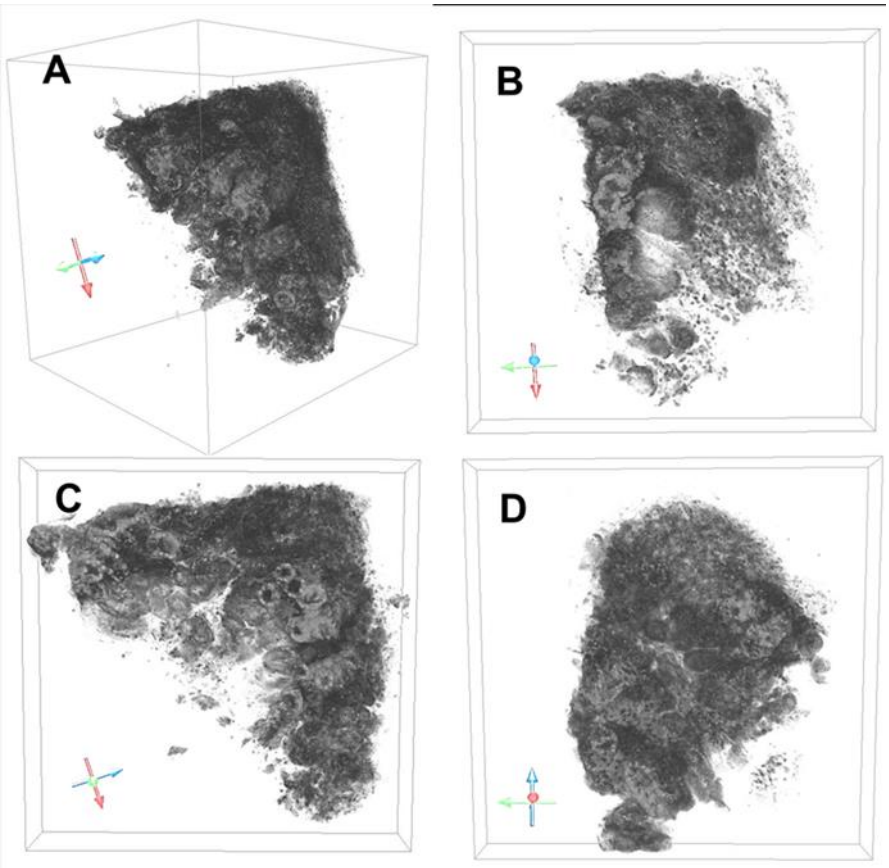

Figure 1. (A) 3D model reconstruction of the digestive gland from animal number 1, in which three thin sections have been extracted using a clipbox along the three orthogonal axes: (B) x-axis, (C) y-axis and (D) z-axis.

The 3D image shown in figure 1A allows to identify the presence of the various compartments of the tissue that are represented in greyscale, according to their density. To grant a different view of the sample, more similar to a standard slice as observed in optical microscopy, in figure 1B, 1C and 1D three virtual slices are reported. They were obtained by cutting the 3D model of the specimen along the x-y, y-z and z-x planes, respectively. These thin sections appear very similar to optical microscopy images of the histological sections, but with a higher resolution and without the need of sample staining. While the 3D X-ray tomography is not capable of identifying the elements that compose a complex sample such as a biological organ, it allows discriminating the different densities inside the volume. This allows the identification of the presence of exogenous materials by looking for elements with much higher densities that, in an organic matrix, are not expected. This procedure is called segmentation and it allows the complete identification of the exogenous material in the three samples analysed in this work

(figure 2). By dramatically reducing the opacity of the sample reconstruction (as seen comparing the left and right images), we are able to visualize and localize the high-density pollutants (red).

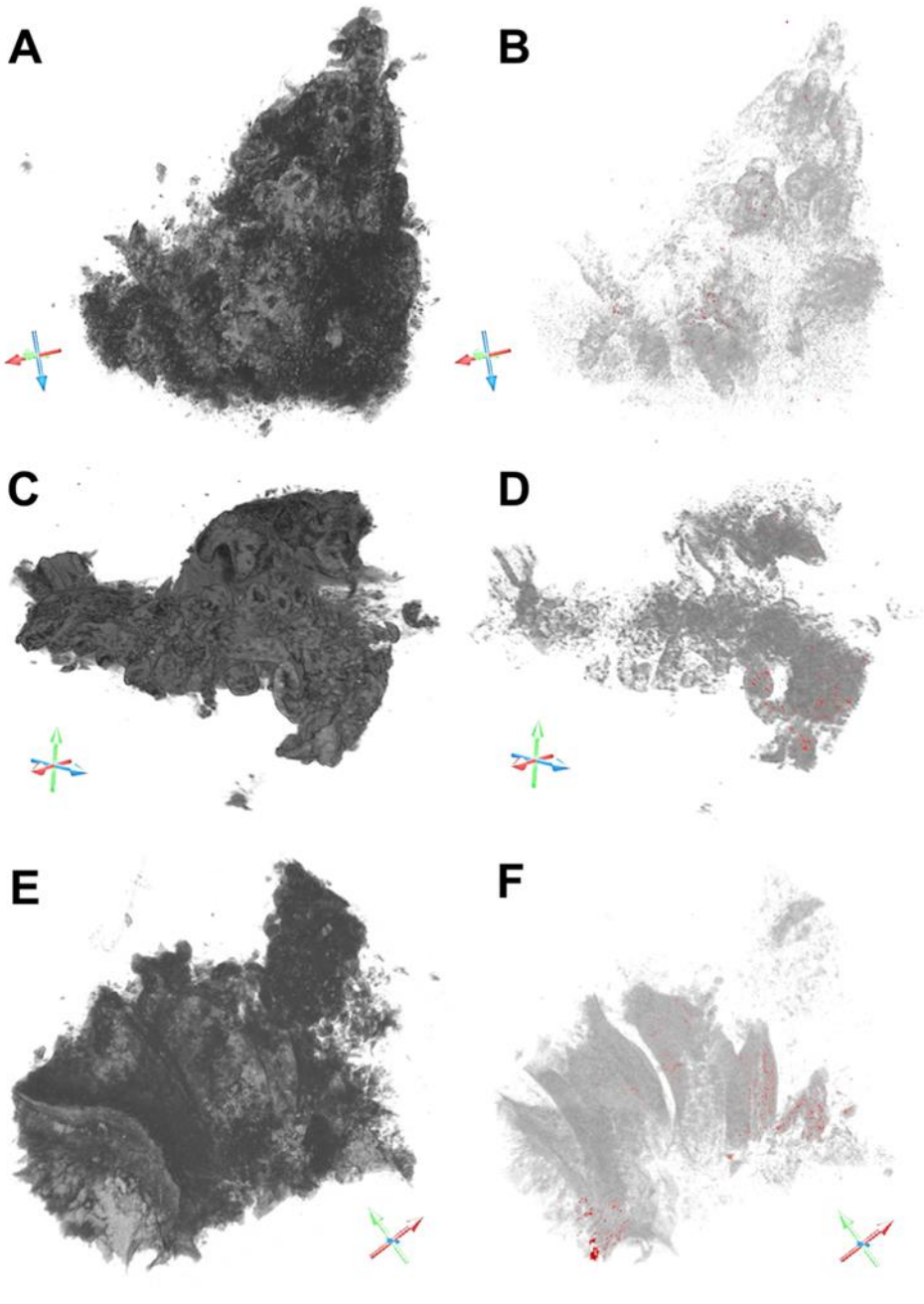

Figure 2. Exogenous pollutants (red) were segmented to highlight their distribution over the whole sample volume after reducing the object's opacity. (A-B) digestive gland from animal 1, (C-D) digestive gland from animal 2 and (E-F) digestive gland from animal 3. There is a preferential distribution of exogenous pollutants inside regions rich in channels and tubules with respect to the connective tissue. A complete segmentation result is shown in figure 3 for the digestive glands of the animal number 2, where the different regions of the organ are mapped in different colours, according to their density.

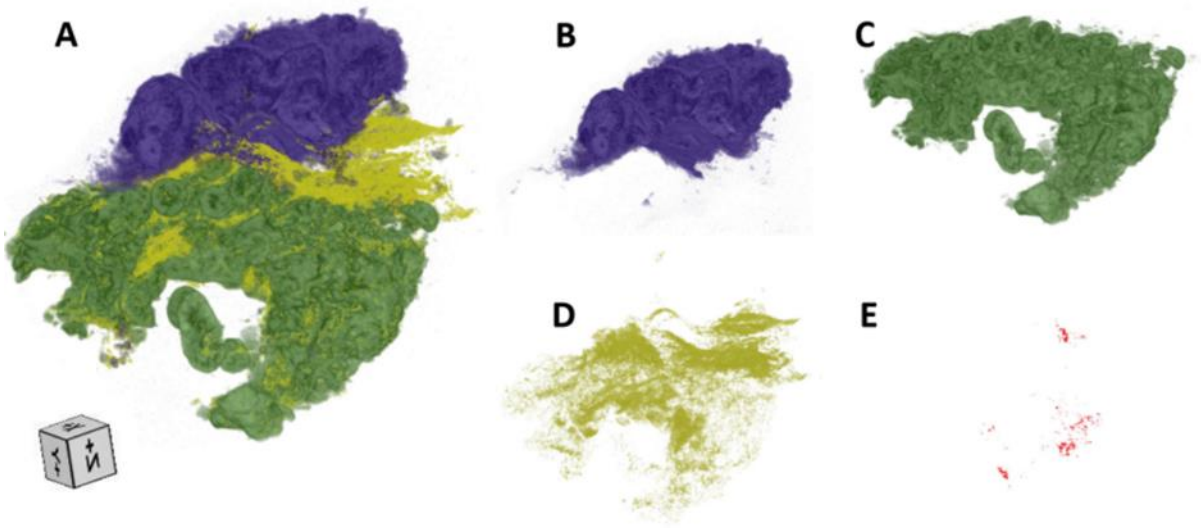

Figure 3. (A) 3D model reconstruction of the digestive gland from animal number 2, where various phases of the organ such as connective tissue, cellular compartment and exogeneous pollutants were segmented. Then, every phase has been extracted and reported separately: (B) high density region rich in tubules and channels, (C) soft density region rich in tubules and channels, (D) connective tissue and (E) exogenous high-density pollutants.

More in detail, in blue (Figure 3B) is shown a high-density region rich in tubules and channels, in green (Figure 3C) is shown a low-density region rich in tubules and channels, in yellow (Figure 3D) is shown a region of connective tissue while in red (Figure 3E) are shown the exogenous materials which exhibit a very high density. From these figures some consideration can be done: (i) the connective tissue connects the two regions of tubules and channels at different densities and (ii) there is a significant presence of exogenous materials that is principally localised in the lower density region. The spatial localization of the technique allows determining that the exogenous materials are not uniformly distributed in the organ; they are not present on the surface of the organ but only inside the channels and tubules (Figure 3A). From these images, it is immediately clear how the segmentation procedure easily and automatically identifies different biological components in the tissue as well as evidencing the exogenous materials. These considerations allow to determine that in all the three organs there is a significant presence of exogenous material that is preferentially localised in the regions rich in channels and tubules, while there is practically no pollutant presence in the connective tissues.
To deal with the quantification of the presence of exogenous materials in the samples, we report in figure 4 their size distributions.

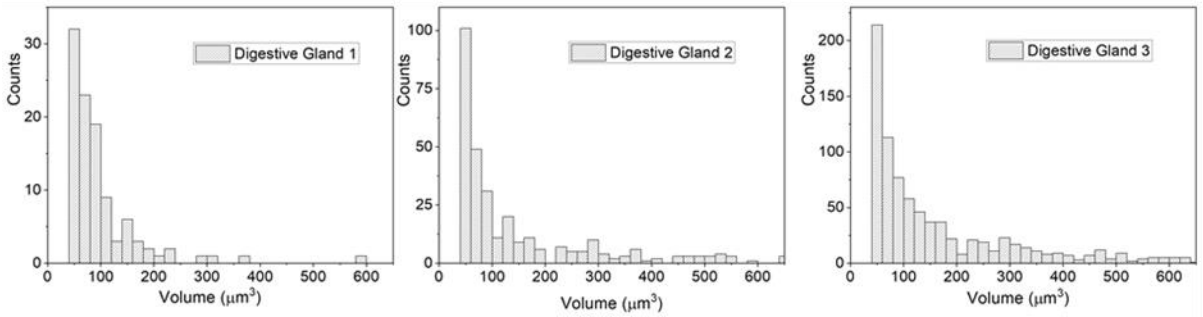

Figure 4. Histograms of the values of the volume of each exogenous material measured in the three samples analysed in this work.

In these histograms are reported the volumes of each single contaminant measured through the segmentation procedures described above. It should be noted that, to comply with the instrumental minimum voxel size of 8 μm^3 and with the necessity of having at least 5 voxels to really identify a single particle, all the contaminants with volume smaller than 40 μm^3 were considered not significant and therefore were removed from the histograms. The shape of the three size distributions appears similar, with a very high peak at lower volumes coupled with the presence of several larger contaminants. The major difference among the samples resides in the total number of contaminants measured, which can depend on several parameters such as the intrinsic different nature of the contamination encountered by the three animals but also by the size of the organ section analysed (i.e., the total volume sampled).

To roughly estimate the sensitivity of our approach we measured the relative volume occupied by the exogenous material, defined by the ratio between the total volume occupied by the exogenous material and the total volume sampled. By this simple calculation we find that this ratio is around 0,004% for sample 1, 0,02% for sample 2 and 0,09% for sample 3. It means that even if the exogenous materials visualized in figures 2 and 3 were widely distributed and clearly visible, their quantity with respect to the entire organ is extremely low, thus highlighting the great sensitivity of this technique, capable to identify and localize highly dispersed components inside very complex and structured specimens.

4. Conclusions

We provided evidence that the 3D X-ray tomography can be a valid tool to identify and localise exogenous materials inside biological specimens, with a micrometric resolution. Such technique can complement other high-resolution approaches such as SEM, TEM and AFM, by providing information on the localization and distribution of contaminants at the level of an entire organ. The key point is the unique capabilities of this technique to provide information on the internal structure of the sample under study, generating a real 3D map of the specimen that can be post-processed by slicing the sample at the desired position focussing directly on the structures of interest. We also demonstrate how the segmentation procedure can be a very powerful tool in discriminating different regions of the sample according to the local density. While this work is not a comprehensive study of the meso-pollutant inside mussel's organ, but a proof of concept of the capabilities of the technique, it shows the capabilities of XRM and its importance in conjunction with other analysis tools. For instance, 3D X-ray tomography could be a first step in a high-resolution approach in the study of contaminants in biological specimens, educating the investigation towards the tissue areas, which could provide the most interesting results using high-resolution or chemically resolved techniques. Once a region of interest packed with exogenous pollutant is observed, correlative microscopy workflows can be exploited to enrich our knowledge with chemical and compositional information down to nanometre scale.

Acknowledgments

This research has been realized with the financial support of the project ATOM (Advanced Tomography and Microscopies), granted by Lazio Region (call "Open infrastructures for research").

References

[1] Griffitt RJ, Luo J, Gao J, Bonzongo JC and Barber DS 2008 Effects of particle composition and species on toxicity of metallic nanomaterials in aquatic organisms *Environmental Toxicology and Chemistry* **27** pp. 1972-1978.
[2] Tangaa SR, Selck H, Winther-Nielsen M and Khan FR 2016 Trophic transfer of metal-based nanoparticles in aquatic environments: a review and recommendations for future research focus *Environmental. Science Nano* **3** pp. 966-981.
[3] Viarengo A and Nott JA 1993 Mechanisms of heavy metal cation homeostasis in marine invertebrates *Comparative Biochemistry and Physiology Part C: Toxicology* **104** pp. 355-372.
[4] Viarengo A, Ponzano E, Dondero F and Fabbri R. 1997 A simple spectrophotometric method for metallothionein evaluation in marine organisms: an application to Mediterranean and Antarctic molluscs *Marine Environmental Research* **44** pp. 69-84.
[5] Rocha TL, Gomes T, Sousa VS, Mestre NC and Bebianno MJ 2015 Ecotoxicological impact of engineered nanomaterials in bivalve molluscs: an overview *Marine Environmental Research* **111** pp. 74-88.
[6] Sousa JC, Ribeiro AR, Barbosa MO, Pereira MFR and Silva AM 2018 A review on environmental monitoring of water organic pollutants identified by EU guidelines *Journal of Hazardous Materialsu* **344** pp. 146-162.
[7] Cravo A, Lopes B, Serafim Â, Company R, Barreira L, Gomes T and Bebbiano MJ 2009 A multibiomarker approach in Mytilus galloprovincialis to assess environmental quality *Journal of environmental Monitoring* **11** pp. 1673-1686.
[8] Gomiero A, Da Ros L, Nasci C, Meneghetti F, Spagnolo A and Fabi G 2011 Integrated use of biomarkers in the mussel Mytilus galloprovincialis for assessing off-shore gas platforms in the Adriatic Sea: results of a two year biomonitoring program *Marine Pollution Bulletin* **62** pp. 2483-2495.
[9] Gomiero A, Spagnolo A, De Biasi A, Kozinkova L, Polidori P, Punzo E, Santelli A, Strafella P, Girasole M, Dinarelli S, Viarengo A, Negri A, Nasci C and Fabi G 2013 Development of an integrated chemical, biological and ecological approach for impact assessment of Mediterranean offshore gas platforms. *Chemistry and Ecology* **29** pp. 620-634.
[10] Dinarelli S, Longo G, Cannata S, Bernardini S, Gomiero A, Fabi G and Girasole M 2020 Metal-based micro and nanosized pollutant in marine organisms: What can we learn from a combined atomic force microscopy-scanning electron microscopy study *Journal of Molecular Recognition* **e2851**.
[11] Duncan KE, Czymmek KJ, Jiang N, Thies AC and Topp CN 2022 X-ray microscopy enables multiscale high-resolution 3D imaging of plant, cells, tissues, and organs *Plant Physiology* **188** pp. 831–845.
[12] Dini D, Cognigni F, Passeri D, Scaramuzzo FA, Pasquali M and Rossi M 2021 Review—Multiscale Characterization of Li-Ion Batteries through the Combined Use of Atomic Force Microscopy and X-ray Microscopy and Considerations for a Correlative Analysis of the Reviewed Data *Journal of The Electrochemical Society* **168** pp. 126522
[13] Carmignato S, Dewulf W and Leach R 2018 Industrial X-Ray Computed Tomography *Springer International Publishing*.
[14] Buzug T and Thorsten M 2008 Computed Tomography: from Photon Statistics to Modern Cone-Beam CT *Springer International Publishing*.
[15] Stock SR 2020 MicroComputed Tomography - Methodology and Applications *CRC Press*.
[16] Reichardt M, Frohn J, Khan A, Alves F and Salditt T 2020 Multi-scale X-ray phase-contrast tomography of murine heart tissue *Biomedical Optics Express* **11** pp. 2633-2651.
[17] Garcea SC, Wang Y and Withers PJ 2018 X-ray computed tomography of polymer composites *Composites Science and Technology* **156** pp. 305-319.